Appendix A. Supplementary Material for “Early diagenetic constraints on Permian seawater chemistry from the Capitan Reef” by Bryant et al.

Table S1 - See attached excel file.

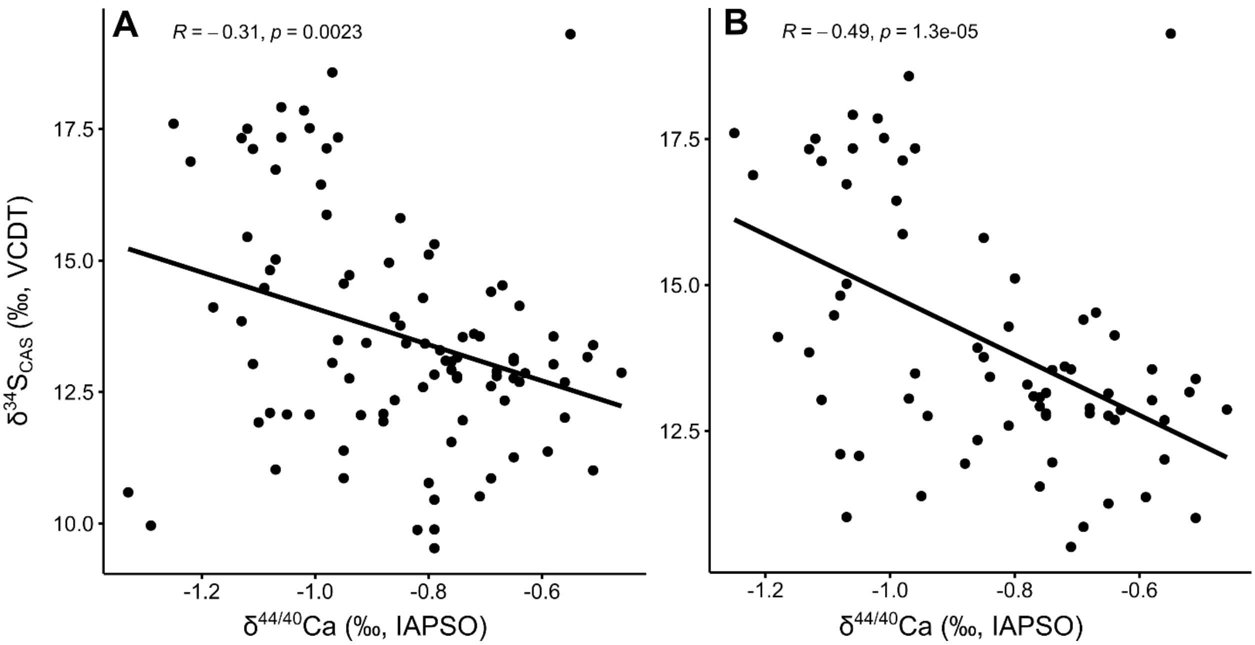

Figure S1. Ca and CAS S isotope data for, (A) non-sparry, calcite-dominated samples, and (B) non-sparry, non-EMC, calcite-dominated samples. The black lines are linear regressions through the data, the Pearson correlation coefficients and p-values for which are shown in the top left corner of the plots.

Sensitivity Analysis

To determine the importance of different variables to the model output (specifically the diagenetic calcite limb in the Ca-S phase space), we conducted a sensitivity analysis, the results of which are detailed below. Generally, all parameters were held constant while one was varied (within a sensible environmental range based on the published literature). The simplest way of quantifying changes in the model output uses the isotopic offsets (here termed ΔCa and ΔS) between the fluid and more sediment-buffered end members (boxes 1 and n in the model). The fluid-buffered end member typically has more positive $\delta^{44/40}$Ca and less positive $\delta^{34}S_{CAS}$ values, whereas the sediment-buffered end member typically has more negative $\delta^{44/40}$Ca and more positive $\delta^{34}S_{CAS}$ values.

Effect of $[SO_4^{2-}]_{seawater}$

The sulfate concentration in the starting fluid ($[SO_4^{2-}]_{seawater}$) has a stark effect on the model output (Figure S2). Raising $[SO_4^{2-}]_{seawater}$ decreases ΔS, mostly by virtue of lowering the $\delta^{34}S$ value of the more sediment-buffered end-member (box n). In other words, sulfate is drawn down more slowly and thus pore fluids become less isotopically evolved over the length of the flow path. Conversely, lowering ($[SO_4^{2-}]_{seawater}$ increases ΔS by increasing the $\delta^{34}S$ value of the more sediment-buffered end-member (box n). This is because sulfate is drawn down more readily, allowing it to evolve more isotopically over the same flow path length.

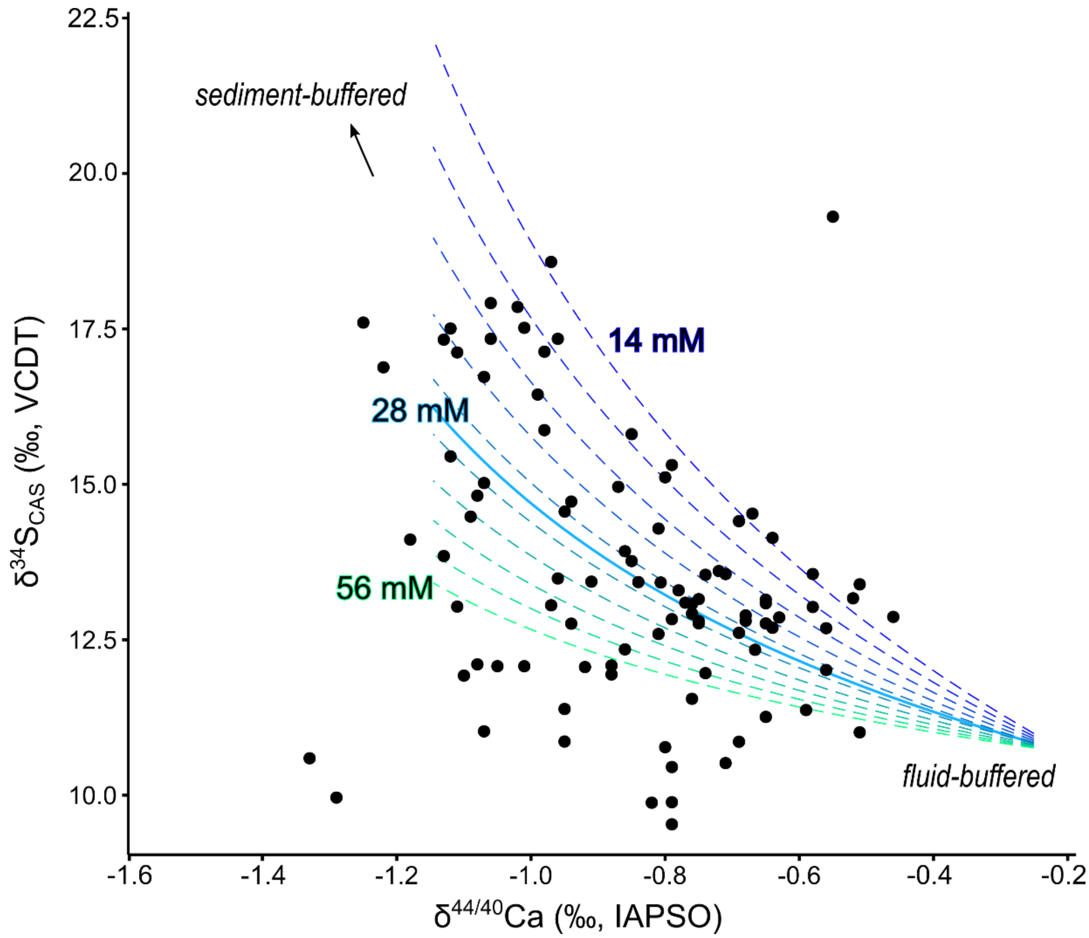

Figure S2. Effect of changing $[SO_4^{2-}]_{seawater}$ on the relative positions of fluid- and sediment-buffered end member diagenetic calcite in the Ca-S isotopic phase space. Black circles are the data from Figure S1A. At a $[Ca^{2+}]_{seawater}$ of 13 mM, a $[SO_4^{2-}]_{seawater}$ of 14 mM gives the best fit between the diagenetic calcite model limb and the upper limb of the data. The dashed lines are at increments of ~4.7 mM between 14 and 56 mM.

Effect of $[Ca^{2+}]_{seawater}$

The calcium concentration in the starting fluid ($[Ca^{2+}]_{seawater}$) has a similarly strong effect on the model output (Figure S3). Raising $[Ca^{2+}]_{seawater}$ decreases ΔCa, mostly by virtue of increasing the $\delta^{44/40}Ca$ value of the more sediment-buffered end-member (box n). In other words, the pore fluids are fluid-buffered over a longer flow path when there is more Ca^{2+} in the incoming seawater. Conversely, lowering ($[Ca^{2+}]_{seawater}$ increases ΔCa by decreasing the $\delta^{44/40}Ca$ value of the more sediment-buffered end-member (box n).

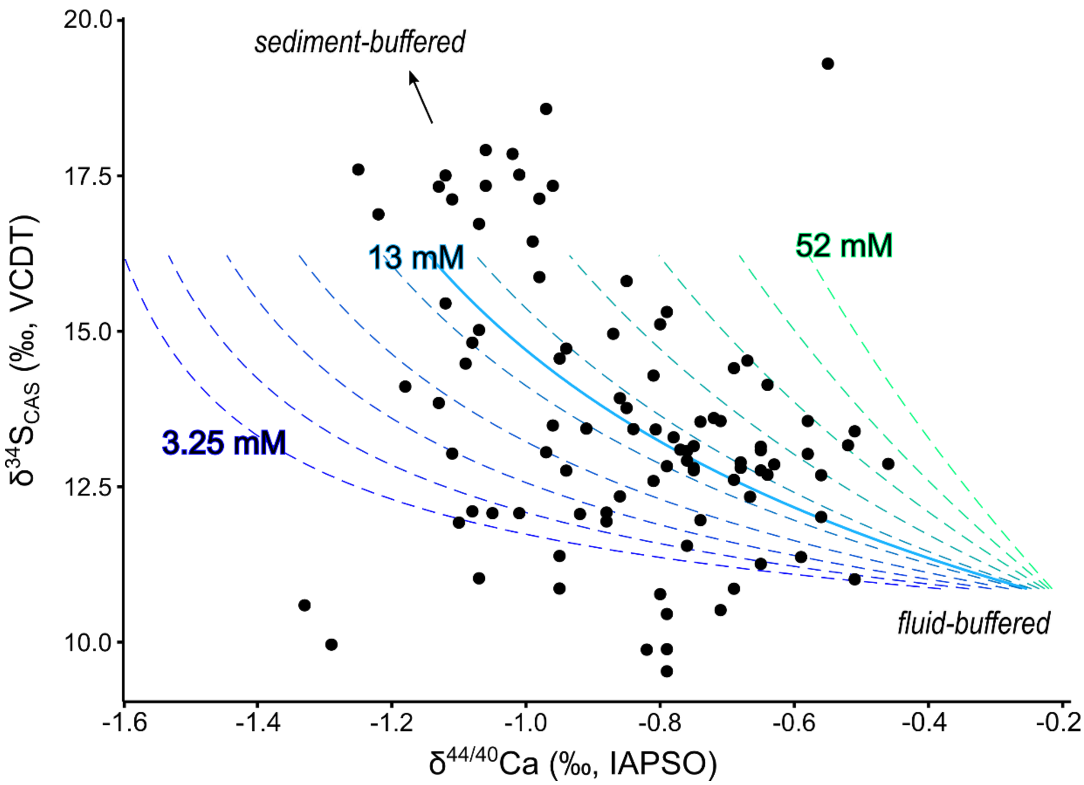

Figure S3. Effect of changing $[Ca^{2+}]_{seawater}$ on the relative positions of fluid- and sediment-buffered end member diagenetic calcite in the Ca-S isotopic phase space. Black circles are the data from Figure S1A. At a $[SO_4^{2-}]_{seawater}$ of 28 mM, a $[Ca^{2+}]_{seawater}$ of 20-30 mM gives the best fit (in terms of slope) between the diagenetic calcite model limb and the upper limb of the data, but fails to reproduce the full range of ΔCa and ΔS represented in the data. Lowering both $[Ca^{2+}]_{seawater}$ to ~13 mM and $[SO_4^{2-}]_{seawater}$ to 16 mM ensures a fit to the full range of ΔCa and ΔS represented in the data (see Figure S2). The dashed lines are at increments of ~5.4 mM between 3.25 and 52 mM.

Effect of primary mineralogy (high-Mg calcite vs. aragonite)

The primary mineralogy (high-Mg calcite vs. aragonite) has a great effect on the model output (Figure S4). Compared to starting with aragonite, starting with calcite gives the same ΔS, but much smaller ΔCa, due to the smaller $\delta^{44/40}Ca$ fractionation between primary calcite and fluid (−1.0‰) vs. primary aragonite and fluid (−1.6‰) (Gussone et al., 2005). As a result of this, the recrystallized product of primary calcite has a steeper slope than the recrystallized product of primary aragonite, assuming all other parameters remain equal. For reference, $[Ca^{2+}]_{seawater}$ would need to be 3 mM, rather than 13 mM, for the recrystallized product of primary calcite to have a similar slope (and ΔS and ΔCa) to the recrystallized product of primary aragonite shown in Figure S4.

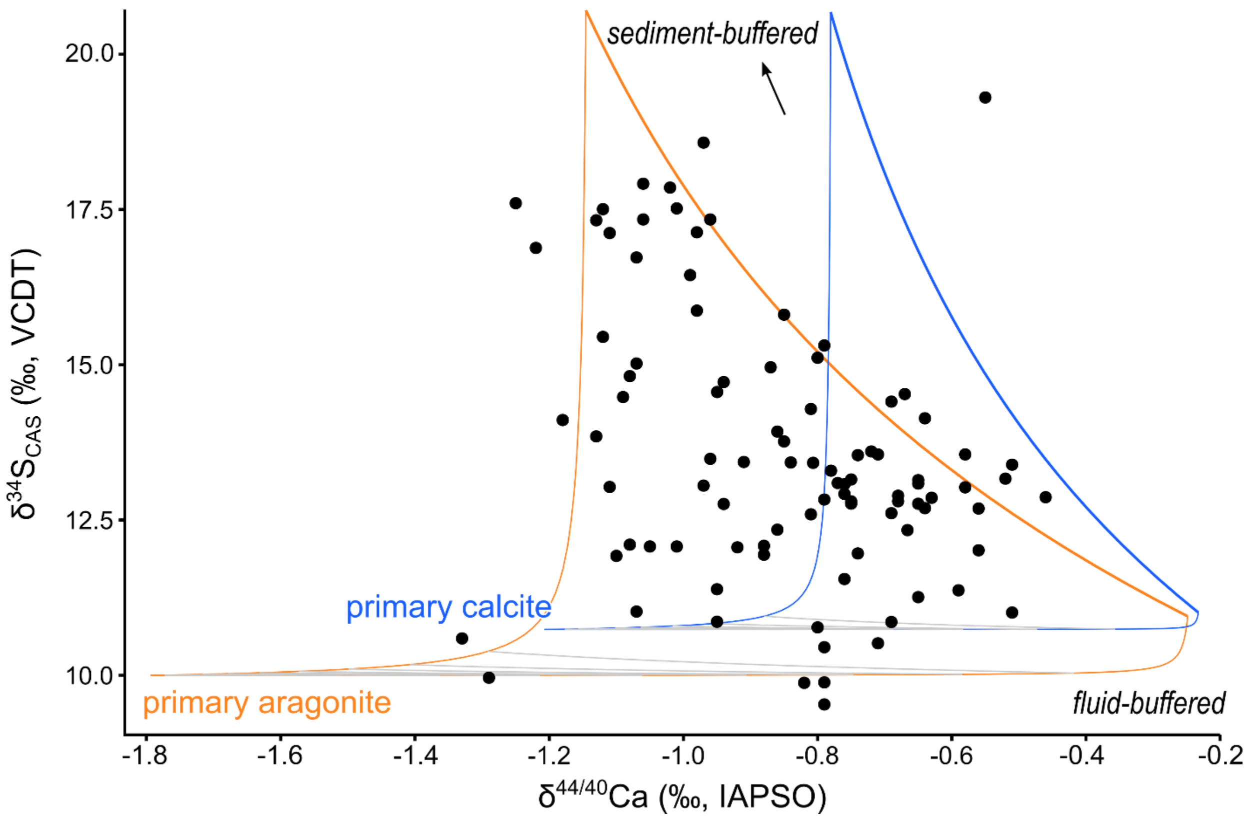

Figure S4. Effect of changing primary mineralogy (calcite vs. aragonite) on the relative positions of fluid- and sediment-buffered end member diagenetic calcite in the Ca-S isotopic phase space. Black circles are the data from Figure S1A.

Effect of organoclastic sulfate reduction rate (MSR rate)

The rate of MSR has a similar effect to $[SO_4^{2-}]_{seawater}$ on the model output. A higher rate results in a higher ΔS by increasing the $\delta^{34}S$ value of the sediment-buffered diagenetic calcite end member (Figure S5). In other words, in a scenario with a high MSR rate, sulfate is drawn down faster, evolves isotopically, and becomes more sediment-buffered along the fluid flow path. In comparison, in a scenario with a low MSR rate, sulfate is draw down more slowly and stays more fluid along the same flow path (n=35).

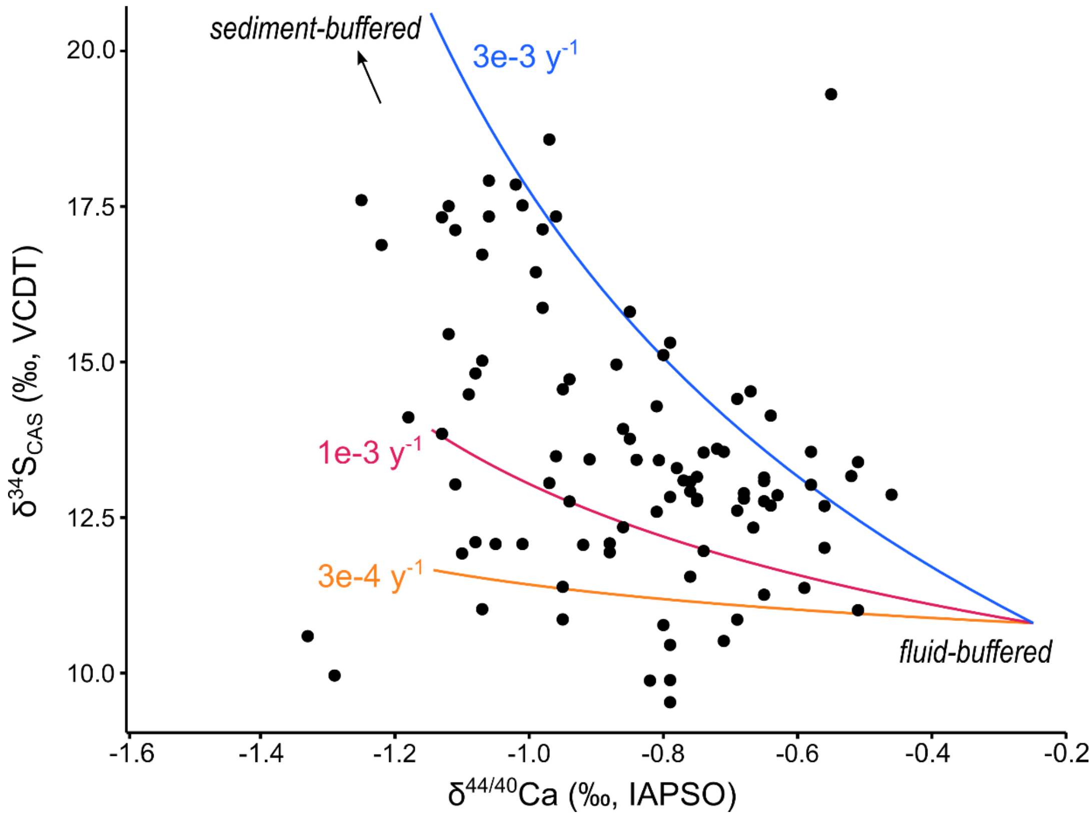

Figure S5. Effect of changing MSR rate on the relative positions of fluid- and more sediment-buffered end member diagenetic calcite in the Ca-S isotopic phase space. Black circles are the data from Figure S1A.

Effect of number of boxes (n)

Adding boxes (i.e., longer fluid-flow path, in meters) to the model increases ΔS and ΔCa, essentially extending the trajectory of the recrystallization deciles (including the 100% diagenetic calcite limb) to more positive $\delta^{34}S_{CAS}$ values and more negative $\delta^{44/40}Ca$, (Figure S6). It is necessary to add enough boxes to the model to span the entire phase-space from fully fluid-buffered to more sediment-buffered in order to capture the data range within (or within instrumental error of) the model output region – in this case 35 boxes were sufficient. The true sediment-buffered endmember (with respect to sulfur) occurs at ~260 boxes, as this length of flow-path is sufficient for the pore water sulfate concentration to be drawn down to zero by the time the primary mineral has completely recrystallized.

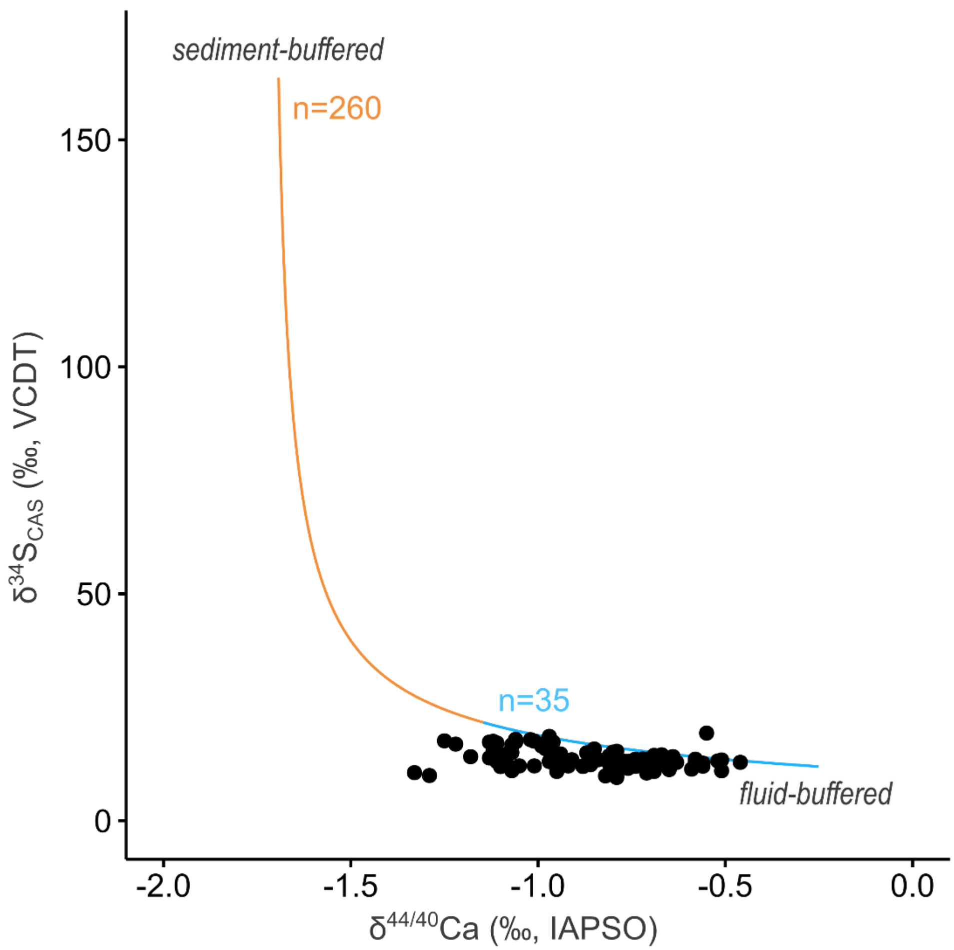

Figure S6. Effect of changing ‘n’ (number of boxes) on the relative positions of fluid- and sediment-buffered endmember diagenetic calcite in the Ca-S isotopic phase space. Black circles are the data from Figure S1A.

Effect of diagenetic ε_{Ca}

Assuming a more negative $\delta^{44/40}$Ca fractionation (ε < 0‰) during recrystallization slightly decreases ΔCa and has no effect on ΔS – this results in a steeper slope. In addition, diagenetic calcite is shifted to more negative $\delta^{44/40}$Ca values. For a $[Ca^{2+}]:[SO_4^{2-}]_{seawater}$ of 0.8125 ($[Ca^{2+}]$ = 13mM; $[SO_4^{2-}]$ = 16mM), most data are fit by assuming ε is 0 to −0.35‰, but some data (mostly EMCs) require ε to be as negative as −0.7‰ (Figure S7).

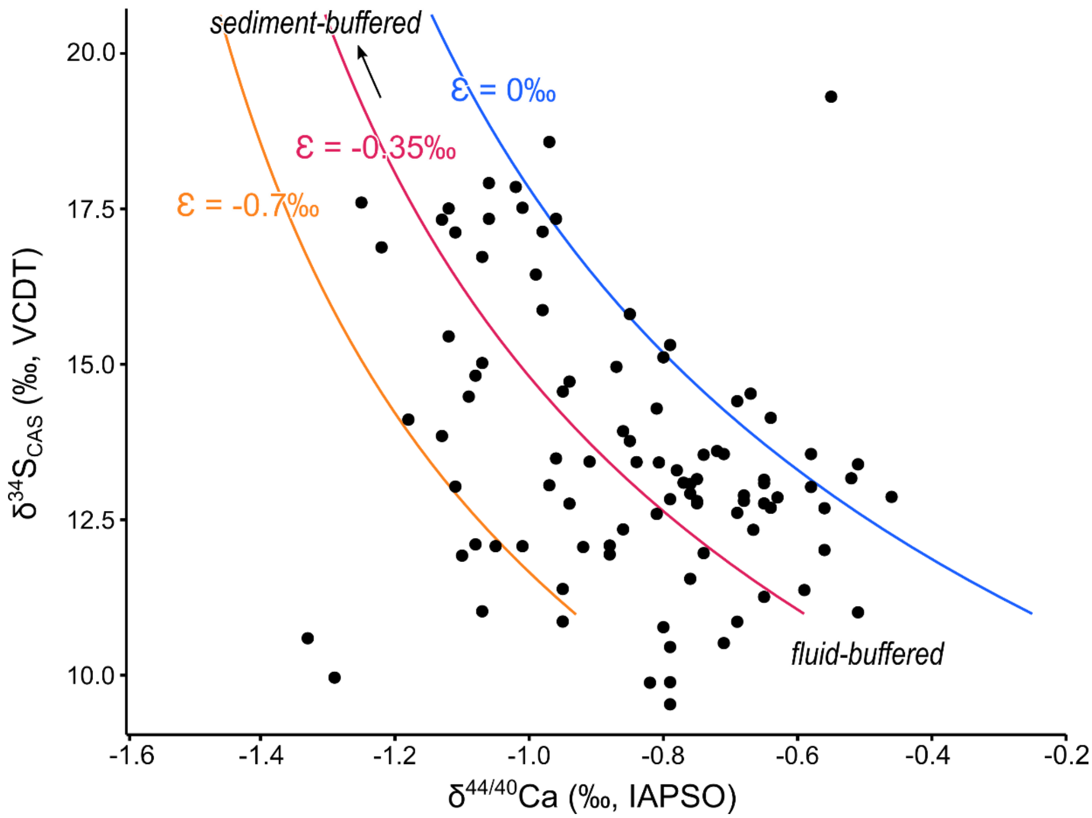

Figure S7. Effect of changing the calcium isotope fractionation factor during recrystallization (ε) on the relative positions of fluid- and sediment-buffered end member diagenetic calcite in the Ca-S isotopic phase space. Black circles are the data from Figure S1.